第35卷第5期
2016年10月

红外与毫米波学报
J. Infrared Millim. Waves

Vol. 35, No. 5
October, 2016

文章编号: 1001 - 9014(2016)05 - 0520 - 06

DOI:10.11972/j.issn.1001 - 9014.2016.05.002

High responsivity of terahertz detector based on ultra-thin $LiTaO_3$ crystal material

LIANG Zhi-Qing[1*], LIU Zi-Ji[1*], JIANG Ya-Dong[1], ZHENG Xing[1], WANG Tao[1], YU He[1]

(1. State Key Laboratory of Electronic Thin Films and Integrated Devices, University of Electronic Science and Technology of China, Chengdu 610054, China)

Abstract: Terahertz (THz) detector work at room temperature could greatly expand the application of THz science and technology. Ultra-thin(10μm) lithium tantalate crystal ($LiTaO_3$) material was used as sensitive layer of the detector. The responsivity could reach up to 8.38×10^4V/W and the noise equivalent power (NEP) could be as low as 1.26×10^{-10}W at 20Hz operating frequency by laser radiation source at 2.52 THz. Furthermore, this processing method to fabricate the ultra-thin $LiTaO_3$ crystal material could potentially provide a feasible approach for even higher response terahertz detectors.

Key words: THz detector, Lithium tantalate ($LiTaO_3$) wafer, chemical grinding and mechanical polishing, Voltage responsivity, noise equivalent power

PACS: 85.25.Pb, 85.60.Gz

基于超薄钽酸锂晶体材料高响应太赫兹探测器

梁志清[1*], 刘子骥[1*], 蒋亚东[1], 郑 兴[1], 王 涛[1], 于 贺[1]

(1.电子科技大学 电子薄膜与集成器件国家重点实验室,四川 成都 610054)

摘要:太赫兹(Thz)探测器工作在室温条件下极大地促进了太赫兹科学与技术的应用。超薄(10μm)钽酸锂($LiTaO_3$)晶片被用作太赫兹探测器敏感元材料。基于钽酸锂晶片太赫兹探测器在2.52 THz激光辐射源照射下,20Hz斩波频率时响应率可达到8.38×10^4V/W,等效噪声功率NEP)可达到1.26×10^{-10}W。这种加工超薄钽酸锂晶片的方法为制备高响应率太赫兹探测器提供了一个可行的方法。

关 键 词:太赫兹探测器;钽酸锂晶片;化学研磨及机械抛光;电压响应率;噪声等效功率

中图分类号:O551,O782 **文献标识码**:A

Introduction

Terahertz (THz) wave is an electromagnetic wave located between microwave and infrared regions of the spectrum spanning from about 0.01mm to 3mm(0.1 ~ 30 THz)[1]. The terahertz region of electromagnetic spectrum is often regarded as the final unexplored area of spectrum and presents a challenge for both electronic and photonic technologies[2-3]. Due to its unique properties, such as low energy, high penetration for some materials and characteristic absorption by large polar molecules, THz detection and imaging technology has huge potential for applying in a variety of fields like information and communication technology (ICT), biology and medical science, radar, electronic warfare, electromagnetic weapons, non-destructive evaluation, homeland security, quality control of food and agricultural products, globe environment monitoring, hidden weapons detection, and so on[4-9].

Received date: 2016-01-06, **revised date**: 2016-04-08 **收稿日期**:2016-01-06, **修回日期**:2016-04-08

Foundation items: Supported by National Science Funds for Creative Research Groups of China (61421002), the National Natural Science Foundation of China (NSFC) (61405027), the China Postdoctoral Science Foundation (2014M562296) and Fundamental ResearchFunds for the Central Universities (ZYGX2011X012)

Biography: LIANG Zhi-Qing(1987-), male, Gansu Huining, Ph. D. Research area involves pyroelectric infrared detectors and terahertz detectors. E-mail: liangzq2012@126.com

* **Corresponding author**: E-mail: liangzq2012@126.com, zjliu@uestc.edu.cn

THz detectors are playing a key role in wide range of these applications[10-14]. The THz detectors can be used for passive or active imaging[15]. Most THz detectors for passive imaging application are highly complex and require extreme cooling working condition[16]. For THz imaging application, it is necessary to develop a compact and portable room temperature terahertz detector. Pyroelectric detectors are excellent candidates for THz detection operating at room temperature. The detectors utilize permanently poled ferroelectric crystals, which generate a charge as the crystal heated up by absorbing incident radiation. The pyroelectric material of lithium tantalate ($LiTaO_3$) has been successfully used in infrared region detection and shows great potentials in the direct detection detectors[17]. However using $LiTaO_3$ material to fabricate THz thermal detector is seldom reported.

1 Experimental results

The typical pyroelectric terahertz detector is structured with $LiTaO_3$ material in the central layer between two metal electrodes. Lithiumtantalate($LiTaO_3$) presents unique electro-optical, acoustic, piezoelectric, pyroelectric and non-linear optical properties[18-23], especially the z-cut single crystal $LiTaO_3$ shows more advantages as a new type of optical material than other traditional optical substrate materials, such as large pyroelectric coefficient, small dielectric constant, high curie temperature and uniformity of crystallinity[24-25]. The two steps in the fabrication of making ultra-thin LT wafer are as follows: mechanical thinning processes and chemical corrosion. 50μm LT wafer can be obtained by grinding and polishing from a single-crystal 200μm thick wafer. After cutting and chemical corrosion process, the thickness of the $LiTaO_3$ could reach up to 10μm[17,26]. To enhance the absorption in terahertz wave, terahertz absorption films are fabricated on the top of the sensitive element surface by its corresponding process. Because the pyroelectric terahertz detector based on $LiTaO_3$ is a kind of thermal detector, the heat conduction is the most important parameter for the performance. The 10μm $LiTaO_3$ layer is presented in Fig. 1(a). The sensitive element structure is shown in Fig. 1(b), from top to bottom individually, there are terahertz gold black absorb coating/dielectric layer/ferrite layer/gold black absorb coating/$LiTaO_3$ crystal (1.2×1.2 mm^2, thickness 10μm)/gold black reflector layer. The electrode structure of sensitive elements is shown in Fig. 1(c). The encapsulation of terahertz detector is shown in Fig. 1(d). To obtain high performance in THz detection, we employ voltage mode to drive the sensitive element, couple with a 100 GΩ resistance and four low noise JFET. The whole elements and circuit are assembled in a TOs39 housing as au integrated device.

We applied all the design parameters to establish the computational mode of the THz detector with optical, thermal and electrical properties as shown in Fig. 1(d). In the simulation, we applied a heat flux of 6.7×10^{-13} W/μm^2 to radiate the detector. The temperature distribution map of the sensitive element is shown in Fig. 2. We evaluated the performance from the simulation results.

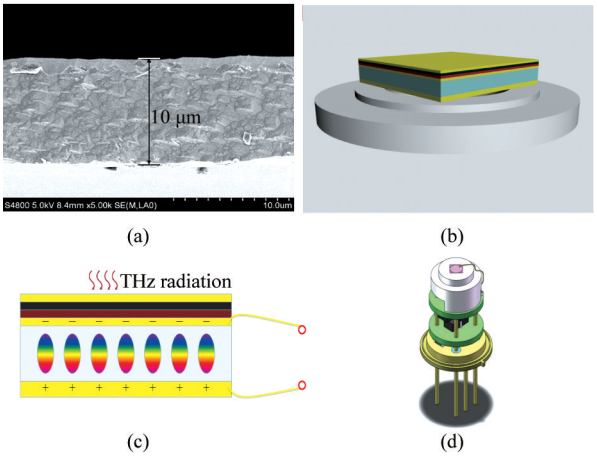

Fig. 1　The device structures of a THz detector, (a) the thickness of the $LiTaO_3$ crystal, (b) sensitive layer structures, (c) electrode structure of sensitive elements, and (d) encapsulation structure of terahertz detector

图 1　太赫兹探测器结构(a)钽酸锂晶片厚度(b)敏感元结构(c)敏感元电极结构(d)太赫兹探测器封装结构

The average increasing temperature is about 3.1mK, and the root mean square (RMS) value of the temperature uniformity is less than 1.1mK. The result is good comparing with some other detectors[26-28].

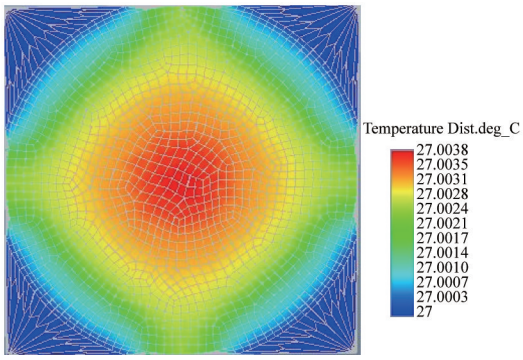

Fig. 2　The temperature changing map at fixed energy flux of the THz detector simulation result of the complex films device structures

图 2　太赫兹探测器复合吸收膜辐射固定能量通量温度变化图

Figure 3 shows the roughness of LT wafer before and after grinding and polishing. It is obvious that the surface scratches are removed by chemical corrosion (Fig. 3(b)).

The biggest challenge in fabricating terahertz detector based on $LiTaO_3$ crystal is highly fragile, which is particularly intrinsic to ultra-thin (10μm) $LiTaO_3$ wafer. In all previous fabrications of the micromechanical terahertz detectors with optical readout, the incident THz radiation goes through the solid Si or SiO_2 substrate[29]. This imposes several limitations on the detector performance. The most significant limitation is related to thermal dissipation. We proposed to surmount this limitation by removing the substrate material underneath the absorbing

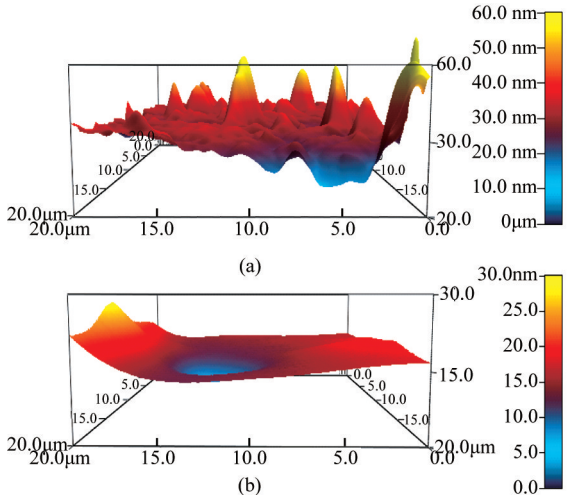

Fig. 3 The roughness of LT wafer (a) before chemical corrosion Ra = 35.466 nm, and (b) after chemical corrosion Ra = 1.462 nm

图3 钽酸锂晶片粗糙度(a)化学腐蚀之前 Ra = 35.466 nm(b)化学腐蚀之后 Ra = 1.462 nm

area of terahertz detector. In order to enhance thermal isolation and electric insulation, we chose a ceramic to chip support the sensitive structure. In addition to providing an unobstructed optical path for THz radiation, this design eliminates the shortest pathway for heat transfer between the absorber and the substrate. Therefore, the thermal isolation of the terahertz detector can be improved.

2 Results and Discussion

One of the important parameters of THz pyroelectric crystal material properties is pyroelectric coefficient[30-32]. As the thickness of LT wafer is 10μm, sensitive area is 1.2 × 1.2 mm^2, the measured pyroelectric coefficient is $P = 4.7 \times 10^{-4}$ C/m^2K[17], the dielectric constant is 44 ~ 53, the density is 7.45 g/cm^3, the roughness is Ra = 1.462 nm and refractive index is n_o = 2.176. The result meets the design requirement of terahertz detector.

The THz detector was fabricated with former pyroelectric materials and simulated structure as shown in Fig. 1(a) and (b), and bonded with pre-amplifier by two spun gold before test as shown in Fig. 1(c) and (d). Because it's a direct detection detector, far infrared laser (the FIR molecule CH_3OH, the pump line is 9P36, radiation frequency is 2.52 THz) acted as terahertz source and oscilloscope was used to display the voltage signal coming from the pre-amplifier. The detecting frequency can be controlled precisely by chopper. The waveform of response voltage signal at 20Hz frequency was shown in Fig. 4. The output waveform from oscilloscope is shown in Fig. 4 (a), and the output waveform from data acquisition card is shown in Fig. 4 (b). The response voltage (Vs) signal and the noise voltage (Vn) of terahertz detector shown in Fig. 5 were measured with lock-in amplifier (SR850) at room temperature after removing ambient radiation. The noise voltage is hundreds of nano-Volts and can be reduced by increasing the test frequency. So we can suppose that it is possible to fabricate high response THz detector based on $LiTaO_3$ crystal.

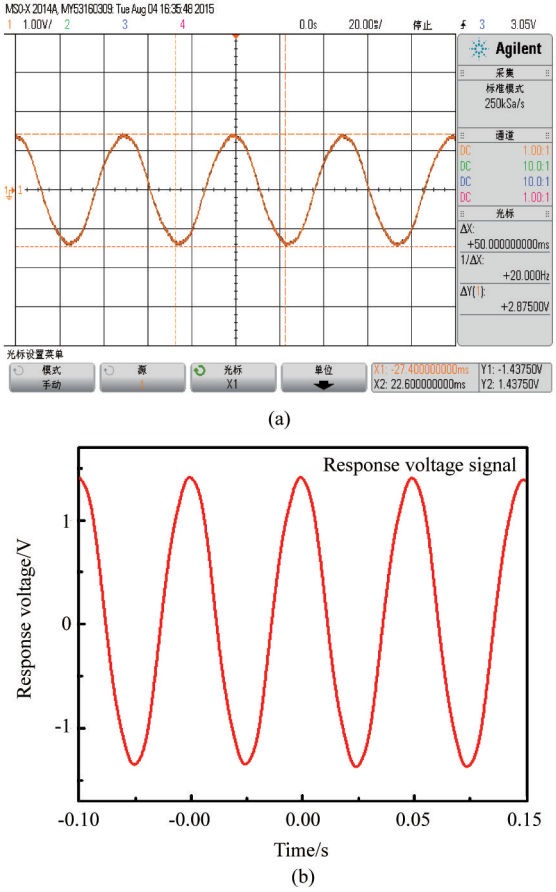

Fig. 4 Output waveform of response voltage signal of THz detector at 20 Hz chopper frequency (a) output waveform from oscilloscope, (b) the output waveform from data acquisition card

图4 太赫兹探测器在20 Hz斩波频率条件下的响应电压输出波形(a)示波器输出波形(b)数据采集卡输出波形

The responsivity (R_v) can be simply expressed as the following equation[33]:

$$R_v = (\eta pAR/G)\omega[1 + \omega^2(RC)^2]^{-1/2}[1 + \omega^2(H/C)^2]^{-1/2} \quad (1)$$

where η is absorptivity of terahertz absorption layer, p is pyroelectric coefficient of $LiTaO_3$ crystal material, A is the area of element, R is the effective resistance in the output circuit of detector and G the effective thermal conductance coupling the detector to a constant temperature heat sink, ω is the operation frequency, C is the electrical and H the thermal capacity of the terahertz detector element. At low operation frequency, for the bulk terahertz detector, the R_v of terahertz detector can be simply modified as shown below[34]:

$$R_v \backsimeq \eta pAR/C_{th} \quad (2)$$

in which, C_{th} is the thermal capacitance and $C_{th} = c_{th}Ad$ (where c_{th} is the volume specific heat, A and d is the area and thickness of the terahertz detector element). As

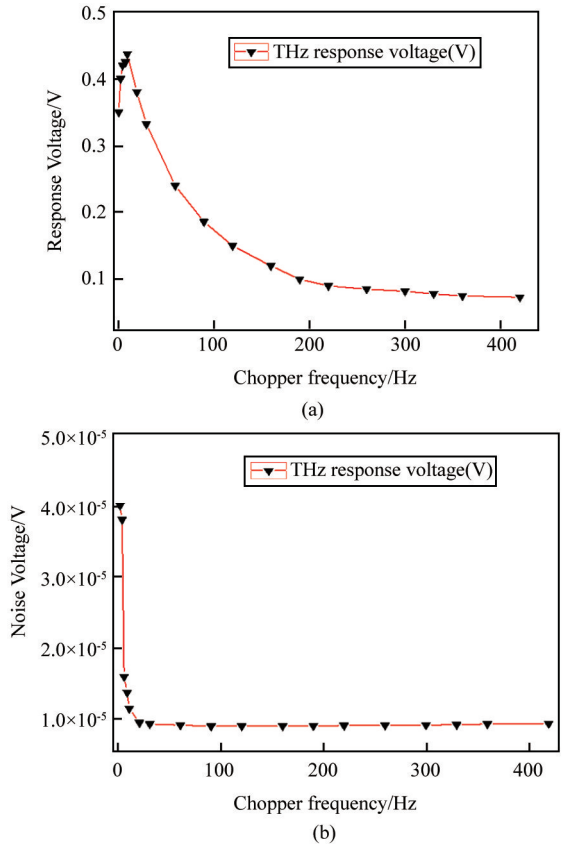

Fig. 5　Response voltage, noise voltage of THz detector at different chopper frequency, (a) output of the response voltage (*Vs*) signal, (b) output of the noise voltage (*Vn*)
图 5　太赫兹探测器在不同斩波频率下响应电压,噪声电压测试结果(a)响应电压(*Vs*),(b)噪声电压(*Vn*)

shown in Eg. 2, the smaller d of $LiTaO_3$ crystal in terahertz detector is , the higher responsivity is. The responsivity depends on the thickness of wafer due to that the thickness affects the thermal capacity of LT wafer[17].

The scratch would bring damage to the crystal surface, and directly influence the subsequent processing of crystal, the application of device performance[17,35], the noise equivalent power value(NEP), and voltage responsivity R_v of the terahertz detector. Chemical corrosion method is used to ensure the uniformity of the polished wafer to enhance the absorption coefficient of a detector with low NEP.

With the value of response, noise, and incident energy, the NEP of terahertz detector can be calculated with the formula as below:

$$NEP = \frac{V_n}{V_s/P} \quad . \quad (3)$$

The value of response and NEP parameters at different frequency of terahertz detector are shown in Fig. 6(b). Obviously, the response for terahertz detector using pyroelectric material reaches 8.38×10^4 V/W and the lowest NEP value reaches 1.26×10^{-10} W at 20Hz operating frequency by using 2.52 THz radiation. This NEP result is superior to other room temperature terahertz detectors[36-41] with NEP about $\sim 10^{-9}$ W. The responsivity of room temperature terahertz detector is higher than other terahertz detectors[42]. The bolometer is a non-coherent detector with the lowest NEP of 10^{-15} W/Hz$^{1/2}$, but it operates at very low temperature and its response speed is slow[43]. Golay cells are room operation, non-coherent detectors with a large spectral response (covering 0.1 ~ 10 THz), a low NEP (less than 10^{-12} W/Hz$^{1/2}$) and a slow response speed. A Schottky diode is an extremely fast, room-temperature THz detector, with a NEP as low as 10^{-12} W/Hz$^{1/2}$. But its response frequency is normally less than 2THz, and its responsivity sharply decreases with increasing THz frequency[44]. Weakly ionized plasma (WIP) detector is an inexpensive THz detector by using the WIP in a neon lamp, its response speed is faster than other THz detector[45], but WIP detector responsivity(44V/W) is lower than terahertz detector using pyroelectric material. The experimental results match the former heat conduction simulation model, which indicates that the conversion ratio from temperature changing to charge of device with $LiTaO_3$ crystal is high. From Fig. 6(a) and 6(b), the NEP parameter of terahertz detector presents an optimizing value near 20Hz chopper frequency, and it increases with frequency. The noise voltage of terahertz detector drops quickly at low frequency, and then it becomes stable at high frequency. The value of V_s

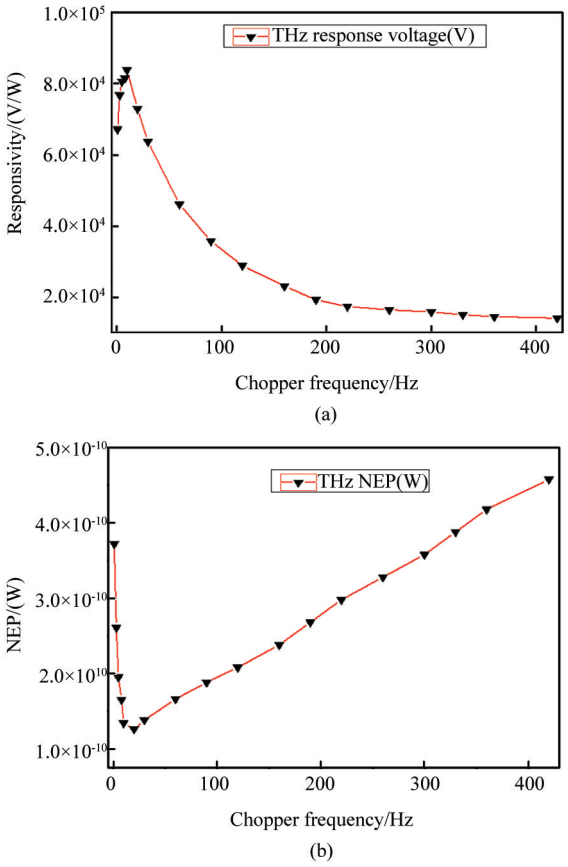

Fig. 6　Responsivity and NEP parameters of THz detector at different chopper frequency (a) responsivity parameters, (b) NEP parameters
图 6　太赫兹探测器在不同斩波频率下响应率和等效噪声功率测试结果(a)响应率参数,(b)等效噪声功率参数

slides down promptly at high frequency, therefore there is an optimizing operating frequency range for those terahertz detectors.

The frequency response graph inset in Fig. 6(a) was also used in order to estimate the quality of the THz detector. The obtained high responsivity (R_v) indicates that the technique can lead to a terahertz testing system with improved performance. More improvements could be achieved by rising the detector's terahertz absorption when an appropriate resonance cavity is embedded into the absorber. We intend to use the layer with thickness optimized so that the absorption is maximized in the terahertz wavelength range.

3 Conclusions

The feasibility of preparing a high responsivity terahertz detector based on ultra-thin (10μm) $LiTaO_3$ wafer is presented in this paper. The responsivity could reach up to 8.38×10^4 V/W. The surface morphology of crystal slice becomes more flat as the thickness reduced to 10μm by oxidizing solution etching. The NEP value of terahertz detector is as low as 1.26×10^{-10} W, which is much better than a detector with others pyroelectric materials.

References

[1] Zeitler J A, Shen Y C. Industrial applications of terahertz imaging [M]//Terahertz spectroscopy and imaging. Springer Berlin Heidelberg, 2012: 451-489.

[2] Siegel P H. Terahertz technology [J]. IEEE Transactions on microwave theory and techniques, 2002, **50**(3): 910-928.

[3] Rogalski A, Sizov F. Terahertz detectors and focal plane arrays [J]. Opto-electronics review, 2011, **19**(3): 346-404.

[4] Asncombe N. No place to hide [millimeter wave imaging] [J]. IEE Review, 2005, **51**(12): 26-30.

[5] Federici J F, Schulkin B, Huang F, *et al.* THz imaging and sensing for security applications—explosives, weapons and drugs [J]. Semiconductor Science and Technology, 2005, **20**(7): S266.

[6] Shin H J, Narayanan R M, Rangaswamy M. Ultra-wideband noise radar imaging of cylindrical PEC objects using diffraction tomography [C]//SPIE Defense + Security. International Society for Optics and Photonics, 2014: 90770J-90770J-10.

[7] Hogbin M. Applying terahertz technology to security [C]//European Symposium on Optics and Photonics for Defence and Security. International Society for Optics and Photonics, 2005: 59891G-59891G-5.

[8] Pickwell E, Wallace V P. Biomedical applications of terahertz technology [J]. Journal of Physics D: Applied Physics, 2006, **39**(17): R301.

[9] Siegel P H, Dengler R J. Terahertz heterodyne imaging Part I: Introduction and techniques [J]. International journal of infrared and millimeter waves, 2006, **27**(4): 465-480.

[10] Kawase K, Ogawa Y, Watanabe Y, *et al.* Non-destructive terahertz imaging of illicit drugs using spectral fingerprints [J]. Optics express, 2003, **11**(20): 2549-2554.

[11] Lee A W M, Hu Q. Real-time, continuous-wave terahertz imaging by use of a microbolometer focal-plane array [J]. Optics letters, 2005, **30**(19): 2563-2565.

[12] Ferguson B, Wang S, Gray D, *et al.* T-ray computed tomography [J]. Optics Letters, 2002, **27**(15): 1312-1314.

[13] Federici J, Moeller L. Review of terahertz and subterahertz wireless communications [J]. Journal of Applied Physics, 2010, **107**(11): 111101.

[14] Siegel P H. Terahertz technology in biology and medicine [C]//Microwave Symposium Digest, 2004 IEEE MTT-S International. IEEE, 2004, **3**: 1575-1578.

[15] Siegel P H, Dengler R J. Terahertz heterodyne imaging Part I: Introduction and techniques [J]. International journal of infrared and millimeter waves, 2006, **27**(4): 465-480.

[16] Cox J A, Higashi R, Nusseibeh F, *et al.* Uncooled MEMS-based detector arrays for THz imaging applications [C]//SPIE Defense, Security, and Sensing. International Society for Optics and Photonics, 2009: 73110R-73110R-11.

[17] Liang Z, Li S, Liu Z, *et al.* High responsivity of pyroelectric infrared detector based on ultra-thin (10μm) $LiTaO_3$ [J]. Journal of Materials Science: Materials in Electronics, 2015, **26**(7): 5400-5404.

[18] Vigouroux H, Fargin E, Gomez S, *et al.* Synthesis and Multiscale Evaluation of LiNbO3-Containing Silicate Glass Ceramics with Efficient Isotropic SHG Response [J]. Advanced Functional Materials, 2012, **22**(19): 3985-3993.

[19] Smith R T, Welsh F S. Temperature dependence of the elastic, piezoelectric, and dielectric constants of lithium tantalate and lithium niobate [J]. Journal of applied physics, 1971, **42**(6): 2219-2230.

[20] Lehman J, Sanders A, Hanssen L, *et al.* Very black infrared detector from vertically aligned carbon nanotubes and electric-field poling of lithium tantalate [J]. Nano letters, 2010, **10**(9): 3261-3266.

[21] Sakamoto W K, Kagesawa S, Kanda D H, *et al.* Electrical properties of a composite of polyurethane and ferroelectric ceramics [J]. Journal of materials science, 1998, **33**(13): 3325-3329.

[22] Chang C C, Chu K P, Lai Y C. The characterization and fabrication of pyroelectric infrared sensor [J]. 淡江理工學刊, 2005, **8**(3): 203-206.

[23] Nougaret L, Combette P, Arinero R, *et al.* Development of ruthenium dioxide electrodes for pyroelectric devices based on lithium tantalate thin films [J]. Thin Solid Films, 2007, **515**(7): 3971-3977.

[24] Wendong Z, Qiulin T, Jun L, *et al.* Two-channel IR gas sensor with two detectors based on LiTaO 3 single-crystal wafer [J]. Optics & Laser Technology, 2010, **42**(8): 1223-1228.

[25] Xu Y. Ferroelectric materials and their applications [M]. Elsevier, 2013.

[26] Wang J, Gou J, Li W. Preparation of room temperature terahertz detector with lithium tantalate crystal and thin film [J]. AIP Advances, 2014, **4**(2): 027106.

[27] Shao X, Ding J, Ma X, et al. Design and thermal analysis of electrically calibrated pyroelectric detector [J]. Infrared Physics & Technology, 2012, **55**(1): 45-48.

[28] He X, Fujimura N, Lloyd J M, *et al.* Carbon nanotube terahertz detector [J]. Nano letters, 2014, **14**(7): 3953-3958.

[29] Grbovic D, Lavrik N V, Rajic S, *et al.* Arrays of SiO2 substrate-free micromechanical uncooled infrared and terahertz detectors [J]. Journal of applied physics, 2008, **104**(5): 054508.

[30] Wood R A. Uncooled thermal imaging with monolithic silicon focal planes [C]//SPIE's 1993 International Symposium on Optics, Imaging, and Instrumentation. International Society for Optics and Photonics, 1993: 322-329.

[31] Rao S S, Sunar M. Piezoelectricity and its use in disturbance sensing and control of flexible structures: a survey [J]. Applied mechanics reviews, 1994, **47**(4): 113-123.

[32] Zhang F X, Sun K. Piezo electrics [M]. 1984: 598-609.

[33] Putley E H. A method for evaluating the performance of pyroelectric detectors [J]. Infrared Physics, 1980, **20**(3): 139-147.

[34] Uchino K. Ferroelectric Devices 2nd Edition [M]. CRC press, 2009.

[35] Fuxing Y. Study on the Ultra-precision Machining Technology for KDP Crystals [J]. Manufacturing Technology & Machine Tool, 2003, **9**: 63-65.

[36] Wang J, Li W, Gou J, et al. Fabrication and parameters calculation of room temperature terahertz detector with micro-bridge structure [J]. Journal of Infrared, Millimeter, and Terahertz Waves, 2015, **36**(1): 49-59.

[37] Spirito D, Coquillat D, De Bonis S L, *et al.* High performance bilayer-graphene terahertz detectors [J]. Applied Physics Letters, 2014, **104**(6): 061111.

(下转第616页)

工作!

References

[1] Seneviratne S I, Corti T, Davin E L, *et al*. Investigating soil moisture-climate interactions in a changing climate: A review[J]. *Earth-Science Reviews*, 2010, **99**(3): 125 - 161.

[2] Price J C. On the use of satellite data to infer surface fluxes at meteorological scales[J]. *J Salmeterol*, 1982, **21**: 1111 - 1122.

[3] Kogan F. Remote sensing of weather impacts on vegetation in non-homogeneous areas[J]. *Int J Remote Sens*, 1990, **11**: 1405 - 1419.

[4] Liu Zhen-hua, ZHAO Ying-shi. Research method of Remote sensing thermal inertia inversion of surface soil water[J]. *China science D: earth science*, (刘振华, 赵英时. 遥感热惯量反演表层土壤水的方法研究. **中国科学 D 辑: 地球科学**), 2006, **36**: 552 - 558.

[5] Hirsave P P, Narayanan P M. Soil moisture estimation models using SIR-C SAR data: a case study in New Hampshire, USA[J]. *Remote Sensing of Environment*, 2001, (75): 385 - 396.

[6] Ulaby F, Sarabandi K, Donald K M, *et al*. Michigan microwave canopy scattering model[J]. *International Journal of Remote Sensing*, 1990, **11**(7): 1223 - 1253.

[7] De Roger R D, Yang D, Ulaby F T, *et al*. A semi——empirical backscattering model at L——band and C - band for a soybean canopy with soil moisture inversion[J]. IEEE Transactions on Geoscience and Remote Sensing. 2001, **39**(4): 864 - 872.

[8] Bindlish R, Thomas J S, Eric W, *et al*. Soil moisture estimates from TRMM Microwave Imager observations over the Southern United States[J]. *Remote Sens Environ*, 2003, **85**: 507 - 515.

[9] Yu Fan, Zhao Ying-shi. A new semi-empirical model for soil moisture content retrieval by ASAR and TM data in vegetation-covered areas[J]. *China Earth: earth science*, (余凡, 赵英时. ASAR 和 TM 数据协同反演植被覆盖地表土壤水分的新方法. **中国科学: 地球科学**), 2011, **41**(4): 532 - 540.

[10] Bindlish R, Barros A P1 Parameterization of vegetation backscatter2 in radar2based, soil moisture estimation[J]. *Remote Sensing of Environment*, 2001, (76): 130 - 137.

[11] Jiménez-Mumoz J C, Sobrino J A, Skokovic D, *et al*. 2014. Land surface temperature retrieval methods from landsat-8 thermal infrared sensor data[J]. *IEEE Geosci. Remote Sens*. Lett., 2014, **11**(10): 1840 - 1843.

[12] Nichol. J. An emissivity modulation method for spatial enhancement of thermal satellite images in urban heat island analysis[J]. *American Society for Photogrammetry and Remote Sensing*, 2009, **75**(5): 547 - 556.

[13] ZHENG Xing-ming, DING Ling-yan, ZHAO Kai, *et al*. Estimation of vegetation water content from Landsat 8 OLI Data[J]. *Spectroscopy and spectral analysis*. (郑兴明, 丁艳玲, 赵凯, 等. 基于 Landsat 8 OLI 数据的玉米冠层含水量反演研究. 光谱学与光谱分析). 2014, **34**(12): 3385 - 3390.

[14] QI Shu-hua, WANG Chang-yao, NIU Zheng. Evaluating soil moisture status in China using the Temperature/Vegetation Dryness Index(TVDI)[J]. *Journal of remote sensing*. (齐述华, 王长耀, 牛铮. 利用温度植被旱情指数(TVDI)进行全国旱情监测研究. **遥感学报**). 2003, **7**(5): 420 - 427.

[15] LI Xin-wu, GUO Hua-dong, LI Zhen, *et al*. Repeat orbit SIR-C polarization interference SAR data of vegetation coverage area of soil moisture inversion study[J]. *Journal of remote sensing*. (李新武, 郭华东, 李震, 等. 重复轨道 SIR-C 极化干涉 SAR 数据植被覆盖区土壤水分反演研究. **遥感学报**). 2009, **13**(3): 430 - 436.

[16] BAO Yan-song, LIU Liang-yun, WANG Ji-hua, *et al*. Estimation of Soil Water Content and Wheat Coverage with ASAR Image[J]. *Journal of remote sensing*, (鲍艳松, 刘良云, 王纪华, 等. 利用 ASAR 图像监测土壤含水量和小麦覆盖度. **遥感学报**). 2006, **10**(2): 263 - 271.

[17] ZHOU Peng, Ding Jian-li, WANG Fei, *et al*. Retrieval methods of soil water content in vegetation covering areas based on multi-source remote sensing data[J]. *Journal of Remote Sensing*. (周鹏, 丁建丽, 王飞, 等. 植被覆盖地表土壤水分遥感反演. **遥感学报**). 2010, **14**(5): 966 - 973.

(上接 524 页)

[38] Wu L, Jiang L, Ding C, *et al*. Effect of Optical Pump on the Dielectric Properties of $LiTaO_3$ in Terahertz Range[J]. *Journal of Infrared, Millimeter, and Terahertz Waves*, 2015, **36**(1): 1 - 6.

[39] Tong J, Huang J, Huang Z, *et al*. Room temperature InGaAs hot electron detector for THz/subTHz regions[C]//Selected Proceedings of the Photoelectronic Technology Committee Conferences held July-December 2013. International Society for Optics and Photonics, 2014: 914202 - 914202 - 7.

[40] Coppinger M J, Sustersic N A, Kolodzey J, *et al*. Sensitivity of a vanadium oxide uncooled microbolometer array for terahertz imaging[J]. *Optical Engineering*, 2011, **50**(5): 053206 - 053206 - 5.

[41] Marczewski J, Knap W, Tomaszewski D, *et al*. Silicon junctionless field effect transistors as room temperature terahertz detectors[J]. *Journal of Applied Physics*, 2015, **118**(10): 104502.

[42] He X, Fujimura N, Lloyd J M, *et al*. Carbon nanotube terahertz detector[J]. Nano letters, 2014, **14**(7): 3953 - 3958.

[43] Tadigadapa S, Mateti K. Piezoelectric MEMS sensors: state-of-the-art and perspectives[J]. *Measurement Science and technology*, 2009, **20**(9): 092001.

[44] Brown E R. A system-level analysis of Schottky diodes for incoherent THz imaging arrays[J]. *Solid-State Electronics*, 2004, **48**(10): 2051 - 2053.

[45] Hou L, Shi W. Fast terahertz continuous-wave detectorbased on weakly ionized plasma[J]. *IEEE electron deviceletters*, 2012, **33**(11): 1583 - 1585.